Orbital nature of the hole-like Fermi surface in superconducting $Ba(Fe_{1-x}Co_x)_2As_2$

B. Mansart,[1] V. Brouet,[1] E. Papalazarou,[1] M. Fuglsang Jensen,[1] L. Petaccia,[2] S. Gorovikov,[2] A. N. Grum-Grzhimailo,[3] F. Rullier-Albenque,[4] A. Forget,[4] D. Colson,[4] and M. Marsi[1]

[1]*Laboratoire de Physique des Solides, CNRS-UMR 8502, Université Paris-Sud, FR-91405 Orsay, France*

[2]*Sincrotrone Trieste, Strada Statale 14 km 163.5, IT-34149 Trieste, Italy*

[3]*Institute of Nuclear Physics, Moscow State University, Moscow 119991, Russia*

[4]*Service de Physique de l'Etat Condensé, Orme des Merisiers, CEA Saclay (CNRS URA 2464), FR-91195 Gif-Sur-Yvette cedex, France*

(Received 26 September 2010; revised manuscript received 13 December 2010; published 28 February 2011)

We report a high-momentum and energy resolution angle-resolved photoemission study of superconducting $Ba(Fe_{1-x}Co_x)_2As_2$. Polarization-dependent measurements performed at low photon energy along high-symmetry directions in the Brillouin zone made it possible to get new insight into the role of the five Fe $3d$ orbitals in the complex electronic structure of this compound close to the Fermi level, in particular, into the nature of the holelike pockets. Two distinct inner α pockets could be disentangled, suggesting that their origin is probably due to hybridized d_{xz} and d_{yz}. We also show that the complex outer β pocket is mainly of d_{z^2} nature, with contributions of other orbitals of different symmetry only in specific points of the Brillouin zone, in the proximity of the $k_z = 1$ $[4\pi/c]$ plane. The identification of a d_{z^2} nature for β contributes to our understanding of the role of electron correlations in 122 pnictide superconductors and of the enhancement of the three-dimensional character of the Fermi surface in Co-doped compounds.

DOI: 10.1103/PhysRevB.83.064516 PACS number(s): 71.20.−b, 74.70.Xa, 79.60.−i

I. INTRODUCTION

The recent discovery of superconductivity in iron pnictide compounds[1,2] has triggered an intense scientific effort to understand the electronic properties of these materials. The reasons for their high critical temperatures (T_c) appear quite different with respect to cuprates, as suggested, for example, by the observation of itinerant magnetism in FeAs-based superconductors. Because of the fact that iron pnictides are multiband systems, their more pronounced three-dimensional character and the role played by electronic correlations are possible keys to explain this difference.[3] Nevertheless, identifying the main physical factors underlying their peculiar behavior is very challenging; in addition, their multiband nature determines a complicated electronic structure close to the Fermi level.

Considering, for instance, the 122 family compounds (doped AFe_2As_2, A=Ba, Sr, Ca, Eu), their density of states close to the Fermi level is dominated by the five Fe $3d$ orbitals, as shown by several theoretical works.[4–9] The Fermi surface is composed of hole pockets around Γ and electron pockets around X, even though the number of pockets is still controversial. There are at least two hole pockets around Γ, predicted to originate mainly from d_{yz} and d_{xz} degenerate orbitals. A third pocket is sometimes predicted,[6,8] but no general agreement exists on its orbital character.

The determination of the band orbital character is complicated because the nature of the holelike pockets strongly depends on their position in k_z. With the support of density functional theory (DFT) calculations,[10] it was found that, in the $k_z = 0$ $[4\pi/c]$ plane, the bands come from d_{xz}/d_{yz} and d_{xy} orbitals, while in the $k_z = 1$ $[4\pi/c]$ plane, they originate from d_{xz}/d_{yz}, d_{z^2}, and d_{xy}; it was also proven that the electronic structure details are very sensitive to the crystallographic structure. Taking into account electron correlations can also strongly affect the computed band positions and orbital character, as shown in Ref. 8, where a Gutzwiller density functional calculation taking into account Hund coupling and Coulomb interactions assigned a d_{z^2} origin to a third outer band in $Ba_{0.6}K_{0.4}Fe_2As_2$. Overall, no clear consensus exists on these issues.

From an experimental point of view, angle-resolved photoelectron spectroscopy[11] (ARPES) can provide useful information on this problem, and it has already been employed in several studies on pnictide compounds; experiments performed on the undoped or electron-doped 122-compound $Ba(Fe_{1-x}Co_x)_2As_2$,[10,12–23] nevertheless, gave conflicting conclusions. Three hole pockets were identified in Refs. 10 and 18 and attributed to d_{xy} and d_{xz}/d_{yz} for the inner pockets and d_{z^2} for the outer pocket, only appearing in the $k_z = 1[4\pi/c]$ plane. On the other hand, in Ref. 13, the authors assigned a d_{xz} and d_{yz} nature to the two inner hole pockets and a $d_{x^2-y^2}/d_{xy}$ to the outer hole pocket. Another recent ARPES study in $Ba_{0.6}K_{0.4}Fe_2As_2$ concluded that the inner hole pockets were intertwined, with their orbital character changing while spanning the (x,y) plane.[24]

Overall, many questions are still open concerning the number and the orbital character of inner and outer hole pockets, and the role of electron correlations in the electronic structure of these materials in the proximity of the Fermi surface.

In this paper, we present the results of a low-photon-energy ARPES experiment on $Ba(Fe_{1-x}Co_x)_2As_2$, which allows us to shine light on these open issues. In particular, we took advantage of an experimental setup providing high-momentum resolution and variable photon polarization to clarify the nature of the $3d$ orbitals constituting the hole pockets, and to explain how the d_{z^2} orbitals are instrumental in applying the effects of correlations to the band structure and in determining its three-dimensional character.

II. EXPERIMENTAL

The experiments were performed on $Ba(Fe_{1-x}Co_x)_2As_2$, $x = 0.07$ and 0.08, which are both superconducting below

$T_c \cong 24$ K, and do not exhibit any magnetically ordered phase.[25] Both doping levels gave similar and consistent results as long as the discussion presented in this paper is concerned. Single crystal samples were grown by the self-flux method[25] and fully characterized prior to our measurements. ARPES experiments were performed on the BaDElPh beamline at the Elettra synchrotron light source.[26] Photons from a figure-8 undulator were dispersed by a normal incidence monochromator in the 5–40 eV range. The photon polarization could be varied from linear horizontal to linear vertical by selecting different undulator harmonics.[26] The photoelectrons were detected with a SPECS Phoibos 150 analyzer, with a typical energy resolution of 5 meV, and an angular resolution of 0.1°. The wave-vector dispersing plane of the hemispherical analyzer was parallel to the photoemission plane (defined by the directions of the incident photons and of the emitted electrons; horizontal in our experimental geometry). Measurements were performed on clean surfaces cleaved *in situ* under ultrahigh vacuum with pressure better than 5×10^{-11} mbar. All the results presented here were obtained at $T = 14$ K. The angle between the incident photons and the emitted electrons was 50°, and the different emission angles [noted θ in Figs. 1(c) and 1(d)] were obtained by rotating the sample. The wave vector and energy conservation rules allow the determination of the in-plane photoelectron wave vector inside the solid as a function of the photon energy $h\nu$ and the emission angle θ by the formula $k_{\parallel} = \sqrt{\frac{2m}{\hbar^2}}\sqrt{h\nu - \phi - E_B}\sin\theta$, where E_B is the electron binding energy and ϕ is the material work function.[11] The maximum emission angle used in the discussed data is 17°, which is needed to observe the outer holelike pocket at $h\nu = 6$ eV.

The crystallographic structure of $Ba(Fe_{1-x}Co_x)_2As_2$ is shown in Fig. 1(a) and the Fe $3d$ orbital's orientation as a function of the crystallographic axes is shown in Fig. 1(b). Two different conventions are used in the literature to describe

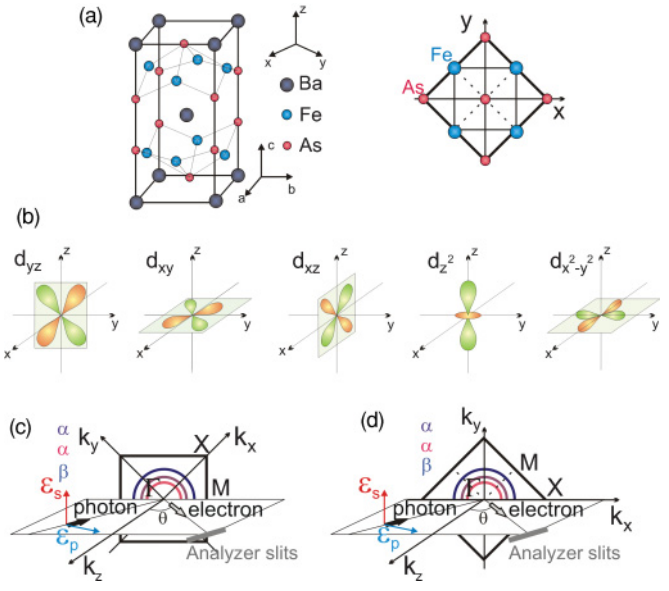

FIG. 1. (Color online) (a) The crystallographic structure of $BaFe_2As_2$ is shown, along with (b) Fe $3d$ orbitals and ARPES geometry in the (c) ΓM and (d) ΓX orientation.

the unit cell of iron pnictides; we chose the one corresponding to a reduced Brillouin zone containing two Fe atoms by unit cell, which we used in this paper. In this notation, the x and y axes are directed toward nearest-neighbor iron atoms, along the iron-iron bonds. We performed ARPES measurements with two different sample orientations, placing either of the two high-symmetry directions of the Brillouin zone (ΓX or ΓM) in the photoemission plane. These two geometries are shown in Figs. 1(c) and 1(d). Furthermore, different k_z planes were explored by tuning the photon energy; therefore, the high-symmetry directions quoted hereafter are parallel to ΓX and ΓM but, in general, not lying in the $k_z = 0[4\pi/c]$ plane. For the sake of simplicity, we will nevertheless refer to them as along ΓX and along ΓM for the specific k_z under study.

III. ARPES MATRIX ELEMENT CALCULATIONS

Polarization-dependent ARPES measurements can give access to the symmetry of the electronic orbitals. The photoemission matrix element within the three-step model approximation is given by the following equation:

$$\left|M_{f,i}^{\mathbf{k}}\right|^2 \propto \left|\langle\phi_f^{\mathbf{k}}|\ \vec{E}\ .\ \vec{r}\ |\phi_i^{\mathbf{k}}\rangle\right|^2, \tag{1}$$

where $\vec{E}$ is the photon electric field and $|\phi_f^{\mathbf{k}}\rangle$ and $|\phi_i^{\mathbf{k}}\rangle$ are the initial and final states of the photoemission process. The values of this matrix element can be calculated as a function of the experimental geometry and photon polarization to obtain the ARPES selection rules,[27] which show that an orbital that is even with respect to the photoemission plane can be detected only with p-polarized photons (p-pol), whereas orbitals that are odd with respect to the photoemission plane will be detected only with s-polarized photons (s-pol); these selection rules are summarized for the iron $3d$ orbitals in Table I. We hereby use the textbook definition for linear photon polarizations: in p-pol, the photon electric field lies in the scattering plane and, in s-pol, its direction is orthogonal to it, as shown in Figs. 1(c) and 1(d). We will hereafter use the subscripts π and σ to indicate bands measured with p-pol and s-pol photons, respectively.

To interpret our ARPES images (shown in Secs. IV and V), we computed the intensity of the photoemission matrix elements within the dipole approximation[28,29] on both sides of the ΓZ direction for $|k_{\parallel}| = 0.18\text{Å}^{-1}$, corresponding to the β band position at the Fermi level. We used a free-electron-like final state and hydrogenlike $3d$ orbitals as initial-state wave functions. Despite the simplicity of this model, we can draw qualitatively interesting conclusions when looking at the sign of the asymmetry, which is defined as the difference in intensity between the band detected at $k_{\parallel} = 0.18\text{Å}^{-1}$ and the band at $k_{\parallel} = -0.18\text{Å}^{-1}$. In particular, we considered the three even

TABLE I. The symmetry of $3d$ orbitals with respect to the photoemission plane (x means neither even nor odd).

Orbitals	d_{z^2}	d_{xy}	$d_{x^2-y^2}$	d_{xz}	d_{yz}	$\frac{d_{xz}+d_{yz}}{\sqrt{2}}$	$\frac{d_{xz}-d_{yz}}{\sqrt{2}}$
ΓX	Even	Odd	Even	Even	Odd	x	x
ΓM	Even	Even	Odd	x	x	Even	Odd

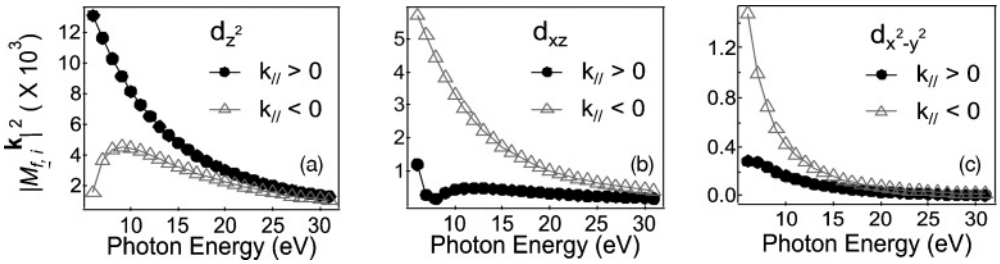

FIG. 2. The angle-resolved photoemission matrix element calculations for the three even orbitals in the ΓX sample orientation.

orbitals potentially observable in p-pol along ΓX; the results as a function of photon energy are shown in Fig. 2. The experimental asymmetry was found to change as a function of photon energy, and to depend on the considered $3d$ orbital. Interestingly, we may notice that the d_{z^2} orbital presents an asymmetry opposed to the other two $d_{x^2-y^2}$ and d_{xz}: it is the only one for which the photoemission yield is larger for $k_\parallel > 0$ than for $k_\parallel < 0$.

IV. ARPES MEASUREMENTS AT $h\nu = 31$ eV

The ARPES results for $Ba(Fe_{1-x}Co_x)_2As_2$, $x = 0.07$, at a photon energy of 31 eV are presented in Fig. 3. In agreement with previous ARPES measurements,[10,12–23] we detect several holelike pockets around the $k_\parallel = 0$ direction. In particular, two bands can be observed, called hereafter α and β, the intensities of which depend on the experimental configuration; the only ARPES image showing a single band is s-pol along ΓM.

The band positions and widths are extracted by fitting the momentum dispersion curves (MDCs), as shown in Figs. 3(c) and 3(f), using Gaussian peaks. We assumed that all bands have approximately the same width, so that broader MDC features required multiple Gaussians to be fitted. Even though one single band may appear broader when, for instance, it becomes flat along the measured direction, this is not the case here (see, for example, the almost linear dispersions observed at $h\nu = 31$ eV in Fig. 3) and we consequently believe that the presence of multiple bands is a reasonable assumption, which (as we shall see) will be corroborated by other results presented later in this paper.

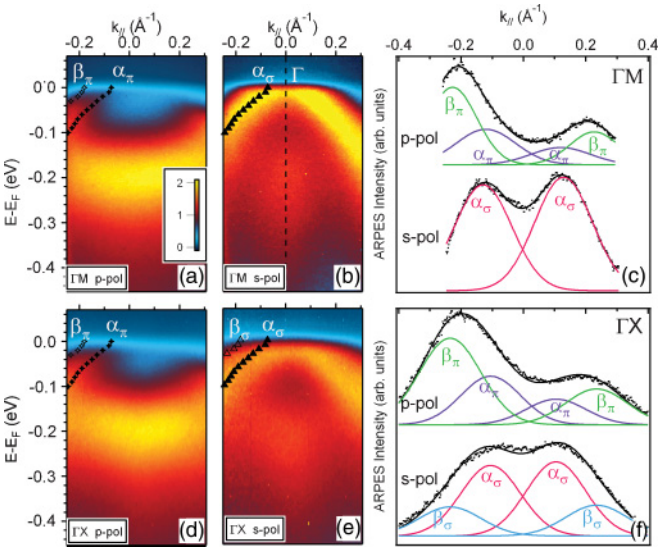

FIG. 3. (Color online) ARPES measurements in different sample orientations and photon polarizations for $x = 0.07$ and $h\nu = 31$ eV. Along ΓM, (a) p-pol, (b) s-pol, and (c) MDCs at $E - E_F = -30$ meV. Along ΓX, (d) p-pol, (e) s-pol, and (f) MDCs at $E - E_F = -30$ meV. The markers in images indicate the band positions extracted from MDC fits, performed as shown in (c) and (f). All images have the same color scale, as shown in (a).

An almost nondispersing spectral feature is visible in Fig. 3 at a binding energy of $E - E_F = -200$ meV in p-pol at $k_\parallel = 0$. It is more than twice more intense in p-pol than in s-pol for both orientations; therefore, it has mainly an even character, which indicates a predominant d_{z^2} origin. This is in agreement with band-structure calculations,[6] even though this band is usually predicted to be more bound (at ≈ -600 meV). However, after renormalization due to the introduction of electronic correlations, bands originating from d_{z^2} can significantly be shifted upward.[8] The same renormalization, mainly attributed to the on-site interorbital Hund coupling J, which is not negligible in these systems, would also be responsible for a strong enhancement of the d_{z^2} character in the outer holelike pocket, called here β. The constraints imposed by lattice-symmetry considerations should also be taken into account. These constraints become particularly evident along high-symmetry directions of the Brillouin zone, giving indications on the possibility for orbitals to hybridize.[11] In the case discussed here, one should note that the ΓZ direction conserves the wave-vector space group $4mm$, in which the d_{z^2} orbital is the only one completely symmetric. This rules out any hybridization between d_{z^2} and other orbitals along ΓZ, which would, for instance, suggest a pure d_{z^2} nature for the nondispersive feature at $E - E_F = -200$ meV.

The outer β band is observed along ΓX for both polarizations, as well as along ΓM in p-pol. This band has a strong even character, and a small odd component along ΓX. In order to match the selection rules of our photoemission measurements, there are several possibilities: (1) β is $\frac{d_{xz}+d_{yz}}{\sqrt{2}}$, so that it is even along ΓM; (2) β has a strong d_{z^2} character, possibly hybridized with other orbitals (d_{xy} or d_{yz}); and (3) β is formed by d_{xy} and $d_{x^2-y^2}$, combined in such a way that its character changes while rotating in the (x, y) plane. The character of β will be further discussed later.

Concerning the inner bands, α_π was measured with p-pol and α_σ with s-pol. Their positions are very close, and they are hardly distinguishable at $h\nu = 31$ eV. If there was only one inner band α, it could be composed of any combination of all of the Fe $3d$ orbitals, because its presence in every experimental configuration would imply no particular symmetry; however,

as we will see later, our low-photon-energy data indicate that there is a small splitting between two inner bands, each of them having a distinct orbital character. Then, following the ARPES selection rules of Table I, α_σ can be composed of d_{xy} or d_{yz} along ΓX and $d_{x^2-y^2}$ or $\frac{d_{xz}-d_{yz}}{\sqrt{2}}$ along ΓM. α_π can be composed of d_{xz}, d_{z^2}, or $d_{x^2-y^2}$ along ΓX and of d_{z^2}, d_{xy}, or $\frac{d_{xz}+d_{yz}}{\sqrt{2}}$ along ΓM. We notice here that a band can change its orbital character while dispersing in the Brillouin zone.

To get deeper insight into this problem, we need to consider other pieces of information, for instance, the asymmetry visible in p-pol ARPES images between positive and negative values of $k_\parallel$ (within the dipole approximation, spectra in s-pol are necessarily symmetric) and the k_z dispersion of the bands. This is the aim of the following section.

V. k_z DISPERSION AT LOW PHOTON ENERGIES

In this section, we present ARPES measurements performed along ΓX on an $x = 0.08$ sample for 6 eV $< h\nu <$ 13 eV. The reduced kinetic energy of the photoelectrons in this photon-energy range makes it possible to perform the measurements with a better wave-vector resolution and with increased bulk sensitivity, which is an important issue in the study of correlated materials.[30] Furthermore, tuning the photon energy makes it possible to obtain detailed information on the orbital character of the bands from their k_z dependence. The k_z is linked to the photon energy through the formula $k_z = \sqrt{\frac{2m}{\hbar^2}}\sqrt{h\nu - \phi + V_0}$, where ϕ is the material work function and V_0 is an inner potential.[11] We used $V_0 = 16.0$ eV in order to match the k_z dispersion, so that the maximum k_F values are obtained for $k_z = 1$ $[4\pi/c]$; in this way, the explored photon-energy range corresponds then to k_z varying from 0.4 to 1.25 $[4\pi/c]$.

The MDCs corresponding to $h\nu = 7$, 9, 11, and 13 eV are shown in Fig. 4 for $E - E_F = -50$ meV. We notice that the choice of a specific binding energy is not critical, and that any value in the range -150 meV $< E - E_F < 0$ leads to the same conclusions as far as the presence or the absence of a band is concerned. The positions of the different bands were extracted by fitting the MDCs at different photon energies as shown in Fig. 3, and their values for 6 eV $< h\nu <$ 13 eV are presented in Fig. 5.

For the sake of comparison, in the same figure we also present the band positions as extracted from the measurements at $h\nu = 31$ eV, which probe the same k_z as 9-eV photons but with a much more pronounced surface sensitivity (the equivalence in k_z of the two photon energies depends of course on the choice of $V_0 = 16.0$ eV and is consequently affected by some uncertainty). The reasonable agreement between the $k_\parallel$ measured at the two different photon energies suggests that no spurious effects related to surface states affect our conclusions. In some cases, structural modulations like the ones due to surface reconstructions modify the band structure,[31] but, in our case, the wave-vector position of the bands is essentially maintained when changing the surface sensitivity of our probe.

The fact that the ARPES intensity shows a different asymmetry in $k_\parallel$ around 9 eV with respect to the data at $h\nu = 31$ eV (comparing, for instance, the p-pol MDCs along ΓX in Figs. 6 and 3) is a strong indication that multiple orbitals contribute to the different bands. Looking at the matrix element calculations presented in Fig. 2, it is clear that only by mixing different orbitals can one reverse the yield between $k_\parallel > 0$ and $k_\parallel < 0$.

In particular, as one can see in Fig. 4, for $h\nu < 13$ eV, β is more intense for positive $k_\parallel$ values. Since d_{z^2} is the

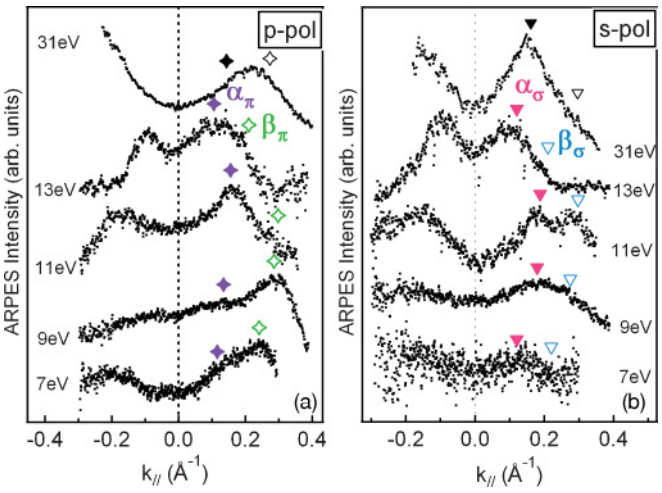

FIG. 4. (Color online) MDCs at $E - E_F = -50$ meV for $Ba(Fe_{1-x}Co_x)_2As_2$ ($x = 0.08$) along ΓX for different photon energies in (a) p-pol and (b) s-pol. The markers indicate the band positions for $k_\parallel > 0$; the positions are identical for $k_\parallel < 0$.

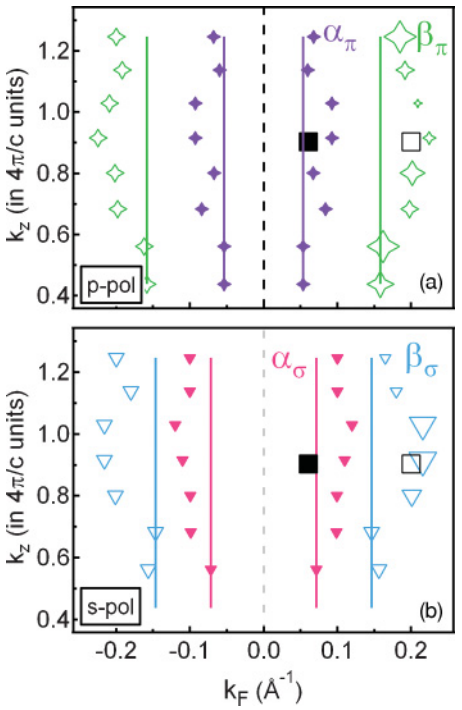

FIG. 5. (Color online) The k_F values (extracted from MDCs at $E - E_F = -10$ meV) for (a) p-pol and (b) s-pol (lines are guides for the eye). The marker weights for $k_F > 0$ (right-hand side) are an indication of the intensity of the β-band signal normalized with respect to the α-band signal. Square markers correspond to the spectra at $h\nu = 31$ eV. The k_z values are given modulo $4\pi/c$.

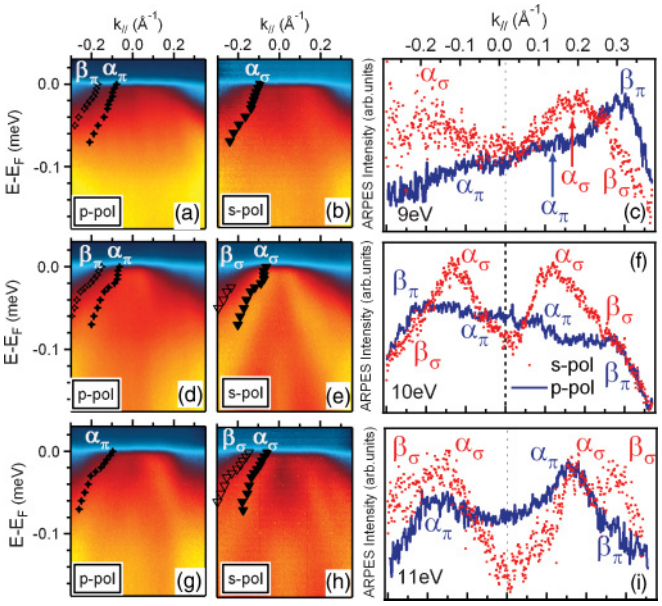

FIG. 6. (Color online) ARPES images and MDCs at $E - E_F = -50$ meV showing the symmetry reversal of β in $x = 0.08$ doped sample along ΓX. (a)–(c) $h\nu = 9$ eV; (d)–(f) $h\nu = 10$ eV; and (g)–(i) $h\nu = 11$ eV. The color scales are similar to Fig. 3.

only d orbital satisfying this condition [see Fig. 2(a)], it must be present in β. At the same time, some hybridization with $d_{x^2-y^2}/d_{xz}$ must be present to explain the asymmetry reversal in ARPES intensity between $h\nu = 31$ eV and around 9 eV. This origin for β is in good agreement with the enhanced k_z dispersion presented by this band, as shown in Fig. 5; in fact, orbitals presenting their lobes out of the (x,y) plane are intrinsically more dispersive along the k_z direction.

Along with this even character with a strong d_{z^2} presence, β presents also some hybridization with other odd orbitals, as visible from the marker's weight in Fig. 5, while β is mainly even over the whole Brillouin zone (from 6 to 9 eV), it becomes markedly odd at 11 eV, which corresponds to $k_z = 1$ $[4\pi/c]$. The comparison between ARPES images and MDCs taken at $h\nu = 9$, 10, and 11 eV are given in Fig. 6, unambiguously showing the change in symmetry of the outer band. This change of symmetry is due to a change of orbital character, from an even orbital (e.g., d_{z^2} and $d_{x^2-y^2}/d_{xz}$) to an odd one (e.g., d_{xy}/d_{yz}).

Let us now turn our attention to the inner bands α. In Fig. 6(c), the arrows indicate the positions of α_π and α_σ extracted from the MDCs at $h\nu = 9$ eV. As one can see, a small but detectable difference in $k_\parallel$ can be observed. We interpret this difference as a splitting between the two inner bands, which has not been clearly reported so far. This can probably be explained by the higher experimental momentum resolution attainable with our measurements at very low photon energies; the splitting is indeed small, and remains difficult to precisely measure in other parts of the Brillouin zone. The overall behavior of the k_z dispersion for α_π, α_σ, and β is summarized in Fig. 5. Although splittings and dispersions are, in some cases, at the limits of detectability, we can nevertheless extract some useful information from the tendencies and the behaviors emerging from Fig. 5.

The fact that α_σ presents a k_z dispersion is in favor of a d_{yz} character for this band. α_π also slightly disperses along ΓX; however, as its intensity is much lower than the β band present in the same images, it is rather difficult to extract k_F values for α_π. Its rather weak dispersive character would be in favor of a $d_{x^2-y^2}$ or d_{xz} origin.

A possibility for the orbital character of α bands would involve only the degenerate d_{xz} and d_{yz} orbitals. α_π could be formed by d_{xz} along ΓX and $\frac{d_{xz}+d_{yz}}{\sqrt{2}}$ along ΓM, while α_σ would be constituted of d_{yz} along ΓX and $\frac{d_{xz}-d_{yz}}{\sqrt{2}}$ along ΓM. This possible scenario would be in agreement with the very close k_F values of these two bands, and with the hypothesis that d_{xz} and d_{yz} orbitals have a strong weight at the Fermi level, due to the enhancement of hopping probability from iron to iron through arsenic atoms, needing free electrons in the d_{xz} and d_{yz} orbitals (for this simplified vision of iron pnictide electronic structure, see, for example, Refs. 5, 32, and 33).

VI. DISCUSSION

In our analysis, we provided information on the orbital character of the holelike pockets along ΓX and ΓM directions. It should be pointed out that a band can change its symmetry while dispersing in the Brillouin zone, and also that the two light polarizations used in our experiments are not enough to pin down undoubtedly the character of each band. Nevertheless, thanks to our matrix element asymmetry calculations and to the observation of a more or less marked k_z dispersion, we may deduce a probable orbital origin for each of the bands.

Some of our conclusions are in agreement with previous ARPES results, in particular, those presented in Ref. 13, but several differences should be pointed out. The most evident one concerns the experimental data, since the β band is observed only very weakly along ΓX in Ref. 13. As far as the discussion is concerned, the claim that the two inner bands α, always present independently of the experimental configuration, are originated from d_{xz}/d_{yz} orbitals is in agreement with our conclusions. Conversely, our analysis and the k_z dispersion we observed with our measurements at low photon energies (see Sec. V) are not compatible with the claim made in Ref. 13 that the β band has a $d_{x^2-y^2}/d_{xy}$ origin and that it presents only a weak dispersion along ΓZ. We may notice that the DFT calculations performed in Ref. 10 show a behavior for the outer band in some sense similar to our experimental results. In Ref. 10, the three bands are shown to be composed mainly of d_{xy}, d_{xz}, and d_{yz} at $k_z = 0$ $[4\pi/c]$, while going to $k_z = 1$ $[4\pi/c]$, they become of d_{xy}, d_{xz}/d_{yz}, and d_{z^2} nature (the latter being the outer band). The fact that several different orbitals have to be taken into account is confirmed by our ARPES study; in particular, a pure d_{z^2} nature can not account for the changes observed during k_z dispersion.

The results on the orbital character of the holelike bands of $Ba(Fe_{1-x}Co_x)_2As_2$, drawn from the data presented here and differing from previous studies, can be summarized as follows:

(1) A small splitting could be observed between the two α inner bands. The outermost one is α_σ, which probably originates from d_{yz} along ΓX and $\frac{d_{xz}-d_{yz}}{\sqrt{2}}$ along ΓM. The

behavior of the innermost one, α_π, is consistent with a d_{xz} origin along ΓX and a $\frac{d_{xz}+d_{yz}}{\sqrt{2}}$ origin along ΓM.

(2) The outer band β has an orbital character depending on the position in the ΓZ direction. It is mainly formed by d_{z^2} along ΓM and ΓX for $k_z \neq 1$ $[4\pi/c]$, hybridized with $d_{x^2-y^2}/d_{xz}$ and d_{xy}/d_{yz}. However, along ΓX, it becomes predominantly formed by d_{xy}/d_{yz} in a range of $\approx \pm 0.1$ around $k_z = 1$ $[4\pi/c]$.

(3) There is an almost nondispersing band centered along ΓZ at a binding energy of ≈ -200 meV, which is mainly formed by d_{z^2} along ΓX and ΓM.

It is worth pointing out that d_{z^2} is the dominating contribution to the outer band β, even though (so far) a d_{z^2} origin for one of the hole pockets rarely emerged from theoretical predictions. It is extremely interesting to notice that, in Ref. 8, the outer band becomes of d_{z^2} character only after introducing electron correlations, and especially the Hund coupling, into their density-of-state calculations. Therefore, the marked d_{z^2} nature of one of the hole pockets represents a very sensitive probe to study the role of electron correlations in $Ba(Fe_{1-x}Co_x)_2As_2$. This aspect deserves further attention and should also be investigated in other iron pnictides such as, for instance, the 11 compounds where electron correlations give more pronounced effects than in the 122 family.

VII. CONCLUSION

In conclusion, the orbital character of the holelike pockets around Γ has been clarified in $Ba(Fe_{1-x}Co_x)_2As_2$. We were able to offer evidence of the presence of several Fe $3d$ orbitals close to the Fermi level in these iron pnictides, elucidating the nature of their complex electronic structure. Thanks to a high experimental momentum resolution at low photon energy, we succeeded in disentangling the two inner α bands, often described as doubly degenerate. They probably originate from d_{xz}/d_{yz} orbitals, in agreement with theoretical predictions. A detailed analysis of the dispersion and the asymmetry in the ARPES yield indicates instead at least a threefold hybridization for the outer band β. It presents a predominant d_{z^2} nature in most of the Brillouin zone, with some hybridization with $d_{x^2-y^2}/d_{xz}$ and d_{xy}/d_{yz}. In particular, along ΓX, its character switches to d_{xy}/d_{yz} in a range of $\approx \pm 0.1$ around $k_z = 1$ $[4\pi/c]$. Our analysis, performed in comparison with the available theoretical models, shows the key role of d_{z^2} orbitals in determining the three-dimensional nature of the Fermi surface of these compounds, as well as in explaining the effects of correlations on the band structure, which are issues of general interest for the physics of superconducting iron pnictides.

ACKNOWLEDGMENTS

The authors gratefully acknowledge D. Malterre for interesting discussions and D. Lonza for his technical assistance during the experiments. The research leading to these results received funding from the European Community's Seventh Framework Programme (FP7/2007-2013) under Grant No. 226716.

[1] Y. J. Kamihara, T. Watanabe, M. Hirano, and H. Hosono, J. Am. Chem. Soc. **130**, 3296 (2008).
[2] M. Rotter, M. Pgerl, M. Tegel, and D. Johrendt, Angew. Chem., Int. Ed. Engl. **47**, 7949 (2008).
[3] I. I. Mazin, Nature (London) **464**, 183 (2010), and references therein.
[4] M. Daghofer, A. Nicholson, A. Moreo, and E. Dagotto, Phys. Rev. B **81**, 014511 (2010).
[5] Y. Ran, F. Wang, H. Zhai, A. Vishwanath, and D-H. Lee, Phys. Rev. B **79**, 014505 (2009).
[6] I. A. Nekrasov, Z. V. Pchelkina, and M. V. Sadovskii, JETP Lett. **88**, 144 (2008) [Pis'ma v Zh. Eksper. Teoret. Fiz. **88**, 155 (2008)].
[7] F.-J. Ma, Z.-Y. Lu, and T. Xiang, Front. Phys. China **5**, 150 (2009).
[8] G. T. Wang, Y. Qian, G. Xu, X. Dai, and Z. Fang, Phys. Rev. Lett. **104**, 047002 (2010).
[9] S. Graser, A. F. Kemper, T. A. Maier, H.-P. Cheng, P. J. Hirschfeld, and D. J. Scalapino, Phys. Rev. B **81**, 214503 (2010).
[10] S. Thirupathaiah *et al.*, Phys. Rev. B **81**, 104512 (2010).
[11] S. Hüfner, *Photoelectron Spectroscopy* (Springer-Verlag, Berlin, 2003)
[12] L. X. Yang *et al.*, Phys. Rev. Lett. **102**, 107002 (2009).
[13] Y. Zhang *et al.*, e-print: arXiv:0904.4022v1.
[14] T. Shimojima *et al.*, Phys. Rev. Lett. **104**, 057002 (2010).
[15] K. Terashima *et al.*, Proc. Natl. Acad. Sci. USA **106**, 7330 (2009).
[16] Y. Sekiba *et al.*, New. J. Phys. **11**, 025020 (2009).
[17] S. de Jong, Y. Huang, R. Huisman, F. Massee, S. Thirupathaiah, M. Gorgoi, F. Schaefers, R. Follath, J. B. Goedkoop, and M. S. Golden, Phys. Rev. B **79**, 115125 (2009).
[18] J. Fink *et al.*, Phys. Rev. B **79**, 155118 (2009).
[19] P. Vilmercati *et al.*, Phys. Rev. B **79**, 220503(R) (2009).
[20] V. Brouet *et al.*, Phys. Rev. B **80**, 165115 (2009).
[21] M. Yi *et al.*, Phys. Rev. B **80**, 174510 (2009).
[22] M. Yi *et al.*, Phys. Rev. B **80**, 024515 (2009).
[23] W. Malaeb *et al.*, J. Phys. Soc. Jpn. **78**, 123706 (2009).
[24] L. A. Wray, D. Hsieh, Y. Xia, S.-Y. Xu, D. Qian, G. F. Chen, J. L. Luo, N. L. Wang, and M. Z Hasan, e-print: arXiv:0912.5089v1.
[25] F. Rullier-Albenque, D. Colson, A. Forget, and H. Alloul, Phys. Rev. Lett. **103**, 057001 (2009).
[26] L. Petaccia, P. Vilmercati, S. Gorovikov, M. Barnaba, A. Bianco, D. Cocco, C. Masciovecchio, and A. Goldoni, Nucl. Instrum. Methods Phys. Res., Sect. A **606**, 780 (2009).
[27] A. Damascelli, Z. Hussain, and Z.-X. Shen Rev. Mod. Phys. **75**, 473 (2003).
[28] F. J. Himpsel, Adv. Phys. **32**, 1 (1983).
[29] R. Matzdorf, Surf. Sci. Rep. **30**, 153 (1998).
[30] F. Rodolakis *et al.*, Phys. Rev. Lett. **102**, 066805 (2009).
[31] R. J. Kelley, Jian Ma, M. Onellion, M. Marsi, P. Alméras, H. Berger, and G. Margaritondo, Phys. Rev. B **48**, 3534 (1993).
[32] Q. Si and E. Abrahams, Phys. Rev. Lett. **101**, 076401 (2008).
[33] S. Raghu, X.-L. Qi, C.-X. Liu, D. J. Scalapino, and S.-C. Zhang, Phys. Rev. B **77**, 220503(R) (2008).